Electrochimica Acta, Vol. 33, No. 8, pp. 1031–1037, 1988.
Printed in Great Britain.

0013–4686/88 $3.00 + 0.00

COMPLEX PROCESSES RELATED TO THE EARLY STAGES OF MERCURY ELECTRODEPOSITION ON Pt ELECTRODES

R. C. SALVAREZZA and A. J. ARVIA

Instituto de Investigaciones Fisicoquimicas Teoricas y Aplicadas, INIFTA, Facultad de Ciencias Exactas, Universidad Nacional de La Plata, C.C. 16, Suc. 4 (1900) La Plata, Argentina

(*Received* 18 *November* 1987; *in revised form* 12 *January* 1988)

Abstract—The underpotential deposition and early stages of bulk mercury electrodeposition on platinum from aqueous solutions containing Hg_2^{2+} ions were studied by using combined potentiostatic and potentiodynamic techniques. The simultaneous electroreduction of the O-containing surface species and the underpotential deposition of Hg_2^{2+} ions render an electrode surface containing an O/Hg atom ratio which depends on both the applied potential and Hg_2^{2+} ion concentration in solution. The nucleation and growth of bulk mercury is impeded by the presence of O-containing surface species, whereas it is markedly enhanced by the presence of Hg-adatoms on the electrode surface. A small number of sites are involved in the nucleation process. Apparently defective points at the UPD Hg layer act as preferred sites for nucleation. It takes potentials more negative than the reversible potential of the Hg/Hg_2^{2+} ion electrode and relatively long electrodeposition times to achieve a degree of surface coverage by mercury atoms greater than 1. It is possible to observe that a fraction of them penetrates into bulk platinum to form a skin-type Hg–Pt alloy.

INTRODUCTION

The stripping processes of Hg which has been underpotential electrodeposited from aqueous mercuric salt solutions on substrates such as Au, Pt and Ir exhibit several voltammetric peaks[1–3], which can be taken as indication of distinguishable Hg electroadsorbates. For both Pt and Au the maximum amount of UPD Hg atoms corresponds to that of a full surface coverage ($\theta = 1$)[1, 2]. There is also evidence that square lattice Hg deposits[4] on Pt lead to a complete monolayer which inhibits entirely the H-adatom electrosorption[2]. On the other hand, when the amount of Hg atoms exceeds the corresponding monolayer charge, they can diffuse into the substrate to form either an alloy, or different intermetallic compounds[1, 2]. In contrast, alloy formation cannot be observed for Hg electrodeposition or Ir electrodes[3].

The nucleation and growth of bulk Hg on Pt was extensively studied by different authors both from experimental and theoretical standpoints[5–10]. The nucleation and 3-D growth processes are inhibited by the presence of oxide layers as the latter reduces the number of preferred active sites available for nucleation[11–12]. As these sites have been associated with holes in the platinum oxide layer the growing bulk Hg phase becomes in direct contact with the Pt substrate. Therefore, for such a complex electrochemical system involving O-adatom stripping yielding bare Pt sites and Hg UPD one can assume that cooperative interactions of different species at the metal surface influence the nucleation and growth of Hg electrodeposits. These types of interactions deserve a detailed consideration as they appear to be extremely important in dealing with the epitaxial growth of metal electrodeposits in aqueous solutions. As a matter of fact, UPD layers of metals may inhibit the nucleation and 3-D growth of foreign metals on different metallic substrates, as it has been reported, for instance, for UPD Pb on polycrystalline Ag where holes existing in the Pb UPD layer become the sites for nucleation and 3-D growth of bulk Pb[13]. In contrast, there was no marked change on the nucleation and 3-D growth of bulk Cu on glassy carbon and graphite by the presence of UPD layers of Cu[14].

The present paper is devoted to investigate Hg UPD and early stages of Hg bulk electrodeposition on Pt to evaluate the influence of Hg UPD and O-adatom stripping on the formation of the metal phase. Results obtained on either polycrystalline or polyfacetted single crystal Pt electrodes in acid solutions covering a wide range of Hg_2^{2+} ion concentration in solution show the influence of UPD atoms, alloy formation and oxide layers on the nucleation and growth of bulk Hg on the different Pt electrode surfaces.

EXPERIMENTAL

The electrodeposition of Hg was performed on polycrystalline (pc) Pt (Johnson Matthey Chemical Co.) and polyfacetted single crystal (pfsc) Pt working electrodes covering from submonolayer range electrodeposits up to few multilayer electrodeposits. The preparation and pretreatment of the working electrodes were reported elsewhere[15]. The apparent electrode surface area was about 0.3 cm^2, and the real electrode surface area was evaluated through the H-adatom electrodesorption charge recorded at 0.1 $V\,s^{-1}$ in 0.5 M H_2SO_4, by taking 210 $\mu C\,cm^{-2}$ for the H-adatom monolayer charge on pc Pt. The potential of the working electrode was measured against a reversible hydrogen electrode in 0.5 M $HClO_4$ and referred to in the text to the standard hydrogen electrode (*she*). A large area Pt sheet was used as counter-electrode. The electrode arrangement was

placed in a conventional three compartment cell. Electrochemical measurements were made at 30 ± 0.1°C in x M $Hg_2(NO_3)_2 + 0.5$ M $HClO_4$ ($10^{-6} \leqslant x \leqslant 10^{-2}$). Solutions were prepared from analytical reagent grade, chemicals and triply distilled water free of impurities. The purity of the solutions was checked through the standing repetitive voltammetric response of the working electrode for at least 30 min at 0.1 V s^{-1} in acid electrolyte in the H-adatom potential range[16]. Single (STPS), repetitive (RTPS) and combined triangular potential voltammograms and potentiostatic current transients were recorded by employing conventional electronic devices referred to in previous works[15]. The various perturbing potential programmes applied to the working electrode were similar to those used in previous works[11, 12].

RESULTS

1. *Basic voltammetric data*

A STPS voltammogram of a pc Pt electrode in 0.5 M $HClO_4$ (Fig. 1, dashed trace) run at $v = 0.1$ V s^{-1} between $E_{s,a} = 1.45$ V and $E_{s,c} = 0.55$ V shows in the electroreduction scan a well-defined cathodic peak (I_c) at 0.79 V due to the electrodesorption of O-containing surface species. The reverse scan depicts a broad and asymmetric peak I_a at 0.87 V related to the formation of O-containing surface species, followed by an apparent current plateau between 1.3 and 1.43 V.

The same electrode in 0.5 M $HClO_4 + 10^{-5}$ M $Hg_2(NO_3)_2$ (Fig. 1, full trace) shows up in the electroreduction scan a slight increase in height and a loss in symmetry of peak I_c, and in the electrooxidation scan a shift for the electroformation of the O-containing surface species towards more positive potentials and a new anodic peak (I'_a) at 1.230 V. As the reversible potential of the Hg/Hg_2^{2+} redox couple, E (10^{-5} M Hg_2^{2+} *vs she*) is 0.640 V, and the charge density of peak I_a is much lower than that of a monolayer for a one electron per site adsorbate, peak I'_a can doubtfully be assigned to the stripping of bulk Hg electrodeposits from the substrate. It appears to be more reasonable to relate peak I'_a to the stripping of a small amount of Hg-adatoms electrodeposited in the potential range of peak I_c. The charge density for Hg stripping estimated from the voltammogram after baseline correction from peak I'_a, is about 70 μC cm^{-2}.

When the $Hg_2(NO_3)_2$ concentration in solution is raised to 3×10^{-4} M, a further increase in height of peak I_c is noticed (Fig. 2). In this case $E_r = 0.685$ V, and the poorly defined peak (II_c) at 0.58 V related to Hg electrodeposition is seen, at potential more negative than E_r, although the complementary stripping peak is not shown up at potentials close to E_r, presumably because of the irreversibility of the process itself. This situation may arise for instance, if the reactant is a Hg–Pt surface alloy instead of bulk Hg atoms. It should also be noticed that the new voltammetric features are accompanied by a large increase in the charge density, $q_{I'_a}$, resulting from peak I'_a, whose value results about 1100 μC cm^{-2}. This charge density includes that related to a monolayer of the O-containing surface species (q_{ox}) which for pc Pt is 420 μC cm^{-2}. Hence, the net charge density assigned to the Hg stripping reaction, ($q_{Hg} = q_{I'_a} - q_{ox}$) becomes 680 μC cm^{-2} thereabouts. Additional aspects of the Hg stripping reaction are presented in the following section.

When the $Hg_2(NO_3)_2$ concentration in 0.5 M $HClO_4$ is raised to 10^{-3} M ($E_r = 0.70$ V) a further increase in the charge of peaks I_c and I'_a can be

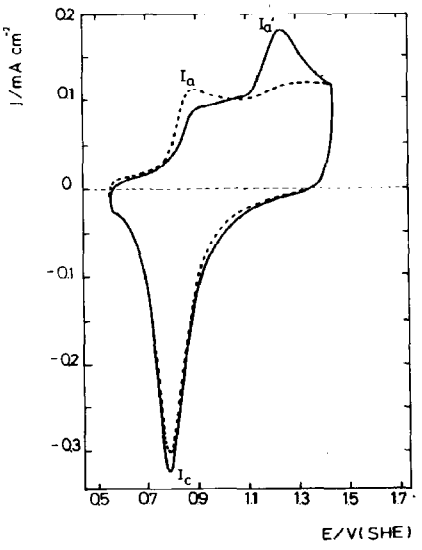

Fig. 1. j/E profiles for pc Pt at $v = 0.1$ V s^{-1} between $E_{s,a} = 1.45$ V and $E_{s,c} = 0.55$ V in (– – –) 0.5 M $HClO_4$ and (——) 0.5 M $HClO_4 + 10^{-5}$ M $Hg_2(NO_3)_2$.

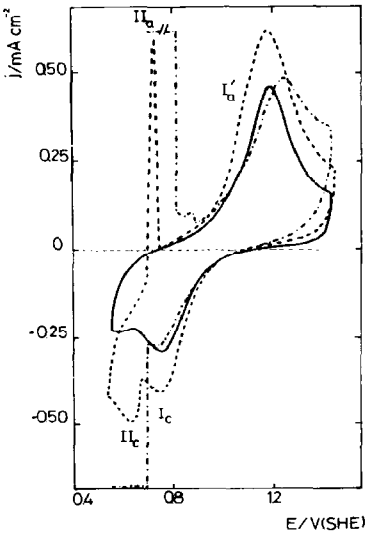

Fig. 2. j/E profiles for pc Pt at $v = 0.1$ V s^{-1} between $E_{s,a} = 1.45$ V and $E_{s,c} = 0.55$ V in 0.5 M $HClO_4$ containing different $Hg_2(NO_3)_2$ concentrations. (——) 3×10^{-4} M, (– – –) 1×10^{-3} M, (–·–·–) 1×10^{-2} M.

observed. Now peak II_c can be clearly seen together with the conjugated very sharp stripping peak II_a corresponding to bulk Hg at 0.72 V. Thus, peak II_c contains two contributions, one coming from the electroformation of a Hg–Pt alloy and another one from bulk Hg electrodeposition. Finally, for $Hg_2(NO_3)_2$ concentrations greater than 10^{-3} M, the contributions of both peaks I_c and I'_a surprisingly start to decrease, in contrast to those of peaks II_c and II_a. These results indicate that peaks I_c and I'_a likely belong to complementary electrochemical reactions, namely, peak I_c should involve the simultaneous electroreduction of O-containing surface species and formation of bare Pt holes where Hg-adatoms are immediately electroadsorbed, and peak I'_a should imply the simultaneous electroformation of O-containing surface species and the Hg electrodesorption. The relative contribution of each one of these processes in the global reaction either cathodic or anodic, apparently changes according to the concentration of $Hg_2(NO_3)_2$ in solution. The general features of these processes resemble to a large extent those recently observed in this laboratory for UPD of Ag on Pt and Rh in acid solutions when these substrates are completely covered by a monolayer of O-containing surface species [15, 17]. Coadsorption and competitive adsorption of Ag and oxygen species were also reported on pc Pt electrodes[18].

2. *The influence of potential holding and* Hg_2^{2+} *ion concentration on the electroformation of* O*-containing surface species on* Pt.

When pc Pt electrodes were held at a constant potential ($E_s = 1.45$ V) for different times ($5\text{ s} \leqslant t_s \leqslant 600$ s) in 0.5 M $HClO_4$ containing different concentrations of Hg_2^{2+} ions, and subsequently subjected to a potential scan at $v = 0.10\ V\,s^{-1}$ from 1.45 V to $E_{s,c} = 0.55$ V, the voltammograms show up a clear dependence on the Hg_2^{2+} ion concentration for any value of t_s (Fig. 3). Thus, for 0.5 M $HClO_4 + 3 \times 10^{-5}$ M $Hg_2(NO_3)_2$ over the entire range of t_s, the charge density related to peak I_c exceeds that recorded for the plain acid solution, but it decreases substantially for 0.5 M $HClO_4 + 3 \times 10^{-3}$ M $Hg_2(NO_3)_2$. These results demonstrate the strong influence of Hg_2^{2+} ion concentration in solution on the amount of O-containing species produced on Pt. In addition, for a constant Hg_2^{2+} ion concentration, the increase in t_s shifts negatively the potential of peak I_c as one should expect when ageing effects related to the formation of the O-containing surface species participate in the entire surface process[12]. Otherwise, the amount of O-containing surface species changes according to t_s.

3. *The influence of surface coverage by* Hg *adatom on the hydrogen electrode reaction on* Pt

From the results described in sections 1 and 2 one can conclude that peak I_c involves two main reactions, namely, the electroreduction of the O-containing surfaces species yielding OH^- ions and bare Pt sites, and the Hg-adatoms electrodeposition on bare sites. Therefore, from these results it is possible to estimate the charge densities, q_{ox} and q_{Hg}, coexisting on the substrate at different potentials and anodization times

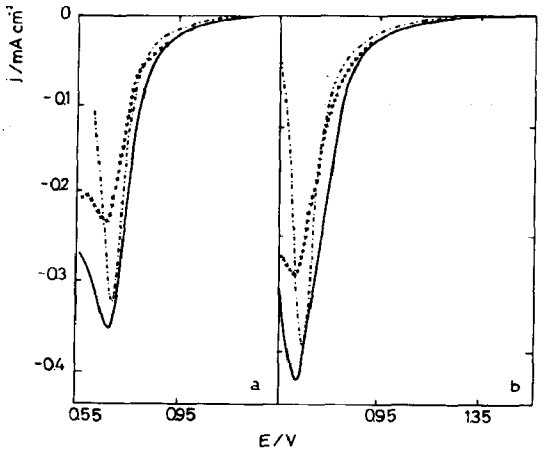

Fig. 3. Cathodic potentiodynamic profiles for pc Pt at $v = 0.1\ V\,s^{-1}$ between $E_{s,a} = 1.45$ V and $E_{s,c} = 0.55$ V after anodization at $E_s = 1.45$ V for different t_s in various electrolytes solutions: (a) $t_s = 10$ s, (–·–·) 0.5 M $HClO_4$, (——) 0.5 M $HClO_4 + 3 \times 10^{-5}$ M $Hg_2(NO_3)_2$, (× × × ×) 0.5 M $HClO_4 + 3 \times 10^{-3}$ $Hg_2(NO_3)_2$; (b) $t_s = 300$ s (–·–·) 0.5 M $HClO_4$, (——) 0.5 M $HClO_4 + 3 \times 10^{-5}$ M Hg $(NO_3)_2$; (× × ×) 0.5 M $HClO_4 + 3 \times 10^{-3}$ M $Hg_2(NO_3)_2$.

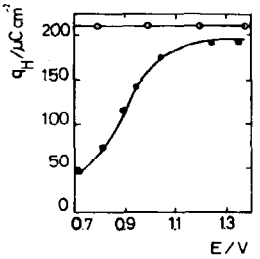

Fig. 4. q_H *vs* E plots in (⊙) 0.5 M $HClO_4 + 10^{-6}$ M $Hg_2(NO_3)_2$ and (●) 0.5 M $HClO_4 + 10^{-4}$ M $Hg_2(NO_3)_2$.

for each electrolyte composition. In order to evaluate the amount of Hg adatoms involved in the potential region of peak I_c, the electrode was firstly anodized at E_s ($0.75\text{ V} \leqslant E_s \leqslant 1.45$ V) during $t_s = 10$ s, subsequently the potential was ramped from E_s to 0 V at $10\ V\,s^{-1}$ for the eventual electroadsorption of H atoms, and immediately afterwards from 0 V upwards at $v = 0.3\ V\,s^{-1}$ to follow the anodic stripping of H-adatoms presumably electroadsorbed in the precedent stage. In this case, the difference between the stripping charge density of H-adatom (q_H) resulting for plain 0.5 M $HClO_4$ and that, q_H, resulting in the Hg_2^{2+} ion containing solutions, can be related to the degree of surface coverage of Pt by Hg-adatoms attained for each solution composition (Fig. 4).

For $Hg_2(NO_3)_2$ concentrations as low as 10^{-6} M, and the entire range of E_s and t_s covered in the present work, the value of q_H results are practically constant and equal to that resulting in the absence of Hg_2^{2+} ions in solution (Fig. 4). This result indicates that for very

low Hg_2^{2+} ion concentrations only negligible amounts of Hg-adatoms are present on the Pt surface probably due to a t_s value too low to reach the adsorption equilibrium. Otherwise, when the $Hg_2(NO_3)_2$ concentration in the acid solution reaches 10^{-4} M, then q_H changes rather sharply with E_s. At $E_s = 0.70$ V, q_H is equal to 50 $\mu C\,cm^{-2}$, and as E_s increases, q_H increases reaching a limiting value of about 190 $\mu C\,cm^{-2}$. It should be noticed that at 0.70 V only a fraction of the O-containing monolayer is still present on Pt. These results clearly demonstrate that bare Pt sites created through the electroreduction of the O-containing surface species are immediately occupied by Hg-adatoms resulting through the Hg_2^{2+} ion discharge. Hence, the Pt surface is always covered by a composite monolayer containing a variable O/Hg atom surface concentration ratio. The latter depends on the applied potential and solution composition, so that the relative O/(O + Hg) and (Hg)/(O) + (Hg) atom surface concentration ratios change either from 1 to 0 or from 0 to 1 respectively, as the O-species stripping process proceeds. Therefore, one should expect a cooperative effect of Hg and O-adatoms on the nucleation and 3-D growth of bulk Hg on the electrode surface as seen in the following section.

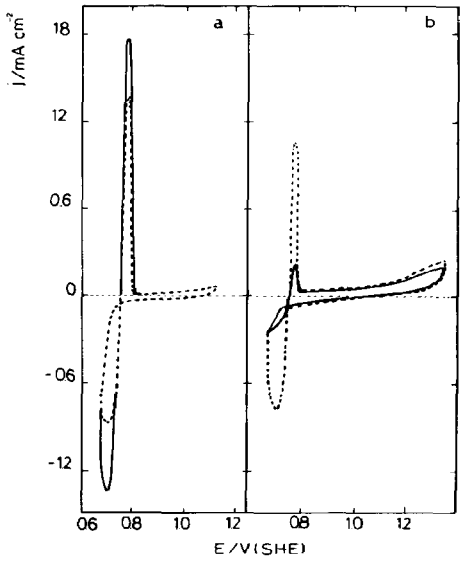

Fig. 5. j/E profiles for pc Pt at $v = 0.1$ V s^{-1} in 0.5 M $HClO_4$ + 1×10^{-2} M $Hg_2(NO_3)_2$ between (a) $E_{s,a} = 1.12$ V and $E_{s,c} = 0.65$ V; (b) $E_{s,a} = 1.35$ V and $E_{s,c} = 0.65$ V. (– – –) First scan, (——) Fifth scan.

4. *Influence of* Hg *and* O-*adatoms on* Pt *on the nucleation and* 3-*D growth of bulk* Hg

The influence of Hg and O-adatoms on Pt on the nucleation and 3-D growth of bulk Hg was mainly followed through potentiostatic current transients and voltammetry in 0.5 M $HClO_4 + 10^{-2}$ M $Hg_2(NO_3)_2$ ($E_r = 0.73$ V). In this case voltammograms were run from 0.65 V to $E_{s,a}$ values positively changed stepwise. Thus, for $E_{s,a}$ lower than $E_{I'_a}$, the potential of peak I'_a (Fig. 5a), the voltammogram shows up a clear cathodic loop (II_c) at potentials close to E_r associated with the nucleation and 3-D growth of bulk Hg and a noticeable peak II_a related to Hg stripping. The potential cycling under these conditions produces a substantial increase in the heights of both loop II_c and peak II_a, as it should occur for an enhancement of Hg electrodeposition. Otherwise, for $E_{s,a} > E_{I'_a}$ (Fig. 5b) the magnitude of loop II_c and stripping peak II_a becomes smaller than that observed for $E_{s,a} < E_{I'_a}$, and, simultaneously peak I'_a, becomes clearer. Finally, for this case, the potential cycling results in a decrease of the pair of peaks II_c–II_a, as one should expect if the simultaneous stripping of Hg-adatom and electroformation of O-containing surface species gradually hinder the nucleation and 3-D growth of bulk Hg.

Reproducible potentiostatic current transients in 0.5 M $HClO_4 + 10^{-2}$ M $Hg_2(NO_3)_2$ were obtained with Pt electrodes previously potential cycled at 0.1 V s^{-1} between 1.45 and 0.65 V, then potential stepped to E_s for $t_s = 300$ s and finally potential stepped to the potential $E_d < E_r$, to record the corresponding current transient (Fig. 6). For $E_s = 0.90$ V, ($E_r \leqslant 0.90$ V $\leqslant E_{I'_a}$), a potential at which the Pt electrode is presumably covered to a large extent by Hg-adatoms, the current transients recorded at E_d decrease initially (not shown in the figure), then increase to reach a maximum current (I_M) at time t_M, and later decays slowly (Fig. 6a). For $E_s = 1.45$ V, a

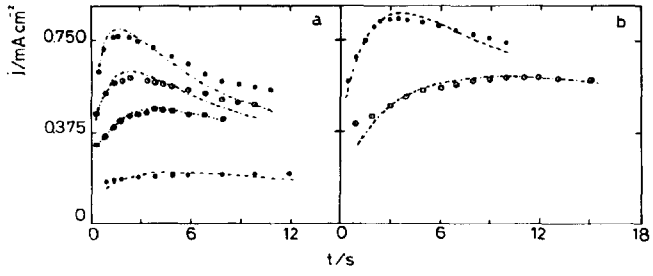

Fig. 6. Current transients at a constant potential ($E_d < E_r$) for pc Pt in 0.5 M $HClO_4 + 10^{-2}$ M $Hg_2(NO_3)_2$. (a) $E_s = 0.90$ V, E_d = (●) 0.718 V, (Θ) 0.723 V, (●) 0.725 V, (O) 0.727 V; (b) $E_s = 1.450$ V, E_d = (O) 0.657 V, (Θ) 0.660 V. Symbols corresponds to experimental data and traces are calculated through Equation (3) and parameters assembled in Table 1.

potential at which both the simultaneous stripping of Hg-adatoms and the electroadsorption of O-adatoms take place, the current transients exhibit the same shape although the overpotential for obtaining a similar bulk Hg electrodeposition charge, turns out to be about 0.06 V higher than that corresponding to E_s = 0.90 V (Fig. 6b). These results firmly indicate that nucleation and growth of bulk Hg is progressively impeded as the surface coverage by O-adatoms increases.

5. *Alloy formation*

The possible formation of a Hg–Pt surface alloy was investigated in 0.5 M $HClO_4 + 10^{-4}$ M $Hg_2(NO_3)_2$ by electrodepositing Hg at a constant potential E_d (0.70 V $\leq E_d \leq$ 0.45 V) on pc Pt electrodes during the time t_d (10 s $< t_d <$ 900 s), and subsequently running an anodic stripping at $v = 0.1$ V s^{-1} between E_d and 1.40 V. Runs comprising E_d values more positive than E_r show up an increase in the height of peak I'_a according to t_d, and for $t_d \to \infty$ a nearly constant charge density value close to 700 μC cm^{-2} is reached. Similar results are obtained with pfsc Pt microelectrodes.

On the other hand, when E_d is set at potentials lower than E_r both the height of peak I'_a and the corresponding bulk Hg stripping charge increase (Fig. 7), with t_d. In this case the charge density resulting from peak I'_a exceeds largely that expected for the sum of Hg and O-adatoms monolayer charge densities which is close to 750 μC cm^{-2}. The same type of experiments made up with pfsc Pt microelectrodes show that the charge of the stripping peak I'_a becomes smaller than that obtained with pc Pt. This means that the structure of the electrode surface plays an important role for the alloying reactions undergoing at $E_d < E_r$.

Current transients were also made by applying to pc Pt electrodes the following potential program: firstly a potential holding at $E_d = 0.45$ V ($E_d < E_r$) during different t_d, then potential stepped to $E_s = 0.80$ V, ($E_r < E_s < E_{I'_a}$), to electrooxidate bulk Hg, and finally potential stepped to 1.45 V for recording the current transient related to stripping peak I'_a. In this case the charge resulting from the current transients increases according to t_d yielding a charge density (q_a) *vs* $t^{1/2}$ linear relationship (Fig. 8). The value of q_a was

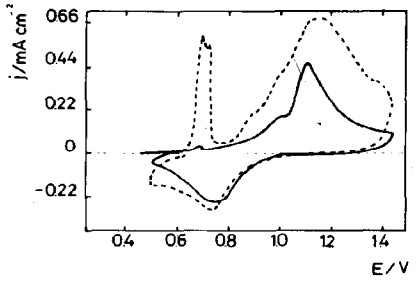

Fig. 7. j/E profiles for pc Pt at $v = 0.1$ V s^{-1} between $E_{s,a}$ = 1.50 V and $E_{s,c}$ = 0.45 V after Hg deposition at E_d = 0.45 V, (——) t_d = 10 s and (– – –) t_d = 90 s, 0.5 M $HClO_4$ + 10^{-4} M $Hg_2(NO_3)_2$.

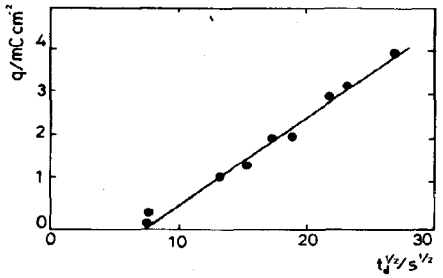

Fig. 8. q_a *vs* $t_d^{1/2}$ plot.

evaluated after considering $q_a = q_{I'_a} - (q_{Hg} + q_{ox})$, and for low Hg_2^{2+} ion concentration the O-adatom monolayer charge density is equal to 420 μC cm^{-2} and q_{Hg} = 330 μC cm^{-2}[19]. From the q_a *vs* $t_d^{1/2}$ plot for t_d = 60 s, it results $q_a = 0$. Accordingly, this value of t_d can be taken as an induction time for alloy formation under the present experimental conditions.

DISCUSSION

1. *Basic phenomenology related to* Hg_2^{2+} *ion electrodeposition on* Pt

The Hg_2^{2+} ion electrodeposition on Pt depends strongly on the value of the applied potential with respect to the reversible potential of the Hg/Hg_2^{2+} redox couple. In principle, the phenomenology of the overall process can be summarized as follows: (i) the electroformation of O-containing surface species on Pt in the presence of Hg_2^{2+} ions in solution is partially inhibited; (ii) the electroreduction of the O-containing surface species leaves bare Pt sites which are immediately filled up with Hg-adatoms through the fast electroadsorption of Hg ions; (iii) the nucleation and 3-D growth of Hg is enhanced when Hg-adatoms are present on the substrate, but it is strongly inhibited when O-adatoms instead of Hg adatoms cover the substrate, and (iv) Hg penetration into bulk Pt yielding a Pt–Hg skin alloy becomes possible when $E_d < E_r$, and t_d exceeds a certain induction time which depends on the electrolyte composition. In order to discuss the entire electrochemical processes let us first consider the reactions undergoing within definite potential ranges.

2. *Electroformation of* O*-containing surface species and* Hg *adatom monolayer*

The voltammetric data indicate that Hg_2^{2+} ions and O-species compete for the electrode surface. At low Hg_2^{2+} ion concentration no marked delayed in the O-adatom electroadsorption can be noticed so that the increase in charge of peaks I_a–I'_a and I_c can only result from the excess of charge coming from the electrodesorption and electroadsorption of the Hg-adatoms on Pt occurring simultaneously with the O-adatom electroadsorption and electrodesorption respectively. Conversely, at relatively high Hg_2^{2+} ion concentration the decrease of peaks I_a–I'_a

and I_c can be assigned to the incomplete stripping of Hg-adatoms. Hence, the number of sites available for the O-electroadsorption becomes smaller than that resulting at low Hg_2^{2+} ion concentration. This explanation is consistent with the increase in the anodic current contribution appearing at the initial portion of the negative potential going j/E scan. This contribution increases according to the Hg_2^{2+} ion concentration in solution (Fig. 2). The simultaneous O-adatom electrodesorption and Hg electrodeposition reactions at the monolayer level also explain the increase in charge of peak I_c as t_s increases (Fig. 3) through the greater coverage of the substrate by O-containing surface species.

The fact that the O-electrodesorption leaves a Pt surface where the progressive suppression of the H-adatom electroadsorption occurs is an indication that bare Pt sites are immediately filled up by Hg-adatoms through the corresponding Hg_2^{2+} ion electroadsorption leading to a Pt surface covered by a composite monolayer containing a variable O/Hg ratio according to the applied potential and solution composition as referred to previously.

3. *Data derived from* Hg–Pt *alloying*

Under the present circumstances alloy formation implies a dynamic behaviour of surface atoms involving either certain defective sites or place exchange processes at the atomic level. In the Hg electrodeposition on Pt, alloy formation is definitely observed only when the Hg adatom monolayer charge has been exceeded, that is $E_d < E_r$.

The average penetration depth (Δx) of the alloy boundary into bulk Pt can be estimated from the equation:

$$\Delta x = Mq_a/zF\rho, \qquad (1)$$

where M and ρ are the atomic weight and the density of mercury respectively, z is the charge involved per atom, and q_a is the stripping charge of the alloy after deposition at E_d for the time t_d. By taking $z = 1$, $q_a = 4000\ \mu C\,cm^{-2}$ ($t = 670$ s), $M = 203\ g\,mol^{-1}$ and $\rho = 13.6\ g\,cm^{-3}$, it results $\Delta x = 3.3$ nm. This figure allows the estimation of D, the diffusion coefficient of Hg atoms into Pt, from the following relationship:

$$(\Delta x)^2 = D' t_d \qquad (2)$$

which yields $D' = 1.6 \times 10^{-16}\ cm^2\,s^{-1}$, in reasonable agreement with the diffusion coefficient reported for metal atoms in solid metal lattices[20].

From the mechanistic standpoint, the growth of the Hg–Pt alloy should involve at least different stages, namely, the initial Hg_2^{2+} ion electrodeposition yielding the Hg-adatom monolayer, followed by the penetration of Hg atoms into bulk Pt, and immediately afterwards the electrodeposition of another Hg_2^{2+} ion on the new Hg–Pt surface. The entire process implies the build up of a concentration gradient of Hg-adatoms from the surface of the substrate inwards. Furthermore, the alloy formation comprises an induction time, which for 10^{-4} M Hg_2^{2+} ion concentration in solution, is in the order of 60 s (Fig. 8b). This means the build up of a certain supersaturation concentration of Hg-adatoms at the Pt surface. On the other hand, the fact that for pfsc Pt alloy formation is slower than for pc Pt indicates that grain boundaries are very likely the preferred paths for Hg atom penetration.

4. *Bulk* Hg *electrodeposition*

The analysis of the current transients recorded for bulk Hg electrodeposition can be used to attempt to clarify the role played by Hg-adatoms and O-containing surface species on the nucleation and 3-D growth process. These current transients can be reasonably simulated by using an instantaneous nucleation and 3-D growth model under diffusion control as previously reported for bulk Hg electrodeposition on other substrates[21]. In this case, at a constant E_d, the instantaneous average current density, $j(t)$, is given by[22]:

$$j(t) = \frac{P_1}{t^{1/2}}[1 - \exp(-P_2 t)] \qquad (3)$$

where $P_1 = zFD^{1/2}c_0/\pi^{1/2}$, $P_2 = \pi K_e D N_0$, $K_e = (8\pi M c_0/\rho)^{1/2}$. D is the diffusion coefficient of Hg_2^{2+} ions in the solution, its bulk concentration is c_0 and N_0 is the number of sites available for nucleation. By using equation (3) and the set of parameters assembled in Table 1, the current transients can be satisfactorily simulated (Fig. 6a and b). From the values of P_2, N_0 can be estimated by taking, for instance, $c_0 = 10^{-5}\ mol\,cm^{-3}$, $D = 10^{-5}\ cm^2\,s^{-1}$, $M = 203\ g\,mol^{-1}$ and $\rho = 13.6\ g\,cm^{-3}$. The values of N_0 depend on the overpotential ($\eta = E_d - E_r$) as seen in Fig. 9. The $\log N_0$ *vs* η plots indicate that nearly the same N_0 value results for Pt surface either highly covered by O-adatoms or covered by Hg-adatoms, despite the fact that the value of η for the former

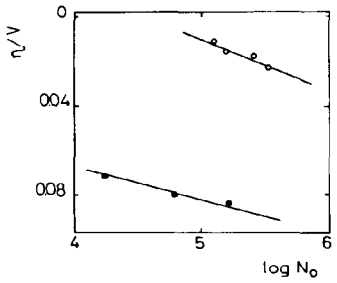

Fig. 9. Log N_0 *vs* η plots, (O) $E_s = 1.05$ V and (●) $E_s = 1.45$ V.

Table 1. Fitting parameters used in Equation (3) for current transients

E_d (V)	P_1 (mA $min^{1/2}\,cm^{-2}$)	P_2 (min^{-1})
$E_s = 0.90$ V		
0.727	0.12	15.07
0.725	0.20	18.87
0.723	0.21	30.15
0.718	0.23	40.14
$E_s = 1.45$ V		
0.660	0.41	5.54
0.657	0.35	21.0

surfaces is appreciably larger than for the latter. As an example, for Hg-adatom covered Pt ($E_a = 0.90$ V), $\eta = 5$ mV, corresponds to a value of N_0 close to 10^5 cm^{-2}, whereas for O-adatom covered Pt ($E_a = 1.45$ V), the value of N_0 resulting by extrapolating to the same η is about 10 cm^{-2}.

It was earlier suggested that holes created either in the UPD Hg layer or in the O-adatom layer could act as preferred sites for nucleation and 3-D growth of the new phase on Pt[11–13]. However, the present results indicate that bulk Hg electrodeposition occurs on a Pt surface covered with a monolayer consisting of different patches whose O/Hg atom surface concentration ratio changes according to both E_d and Hg_2^{2+} ion concentration in solution. In this situation the question arises as to whether bulk Hg electrodeposition takes place at bare Pt sites resulting from the electroreduction of the O-adatom patches (reaction path I) or at defective sites of Hg-adatom patches (reaction path II). On the basis of the complex monolayer structure already discussed, and undergoing reactions, one should expect for reaction path I that the presence of O-adatom patches enhance nucleation and 3-D growth of the bulk Hg, whereas the reverse effect should occur for the Hg-adatom patches. Hence, for reaction path I, at the applied potential E_d ($E_d < E_r$), active sites should be produced through the electroreduction of O-containing surface patches whereas the Hg-adatoms patches become inactive areas for bulk Hg electrodeposition. The fact that the opposite behaviour is observed suggests that Hg-adatoms actually enhance the earlier stages of Hg electrodeposition, that is reaction path II prevails as it was already discussed. Furthermore, it should be noticed that the value of N_0 for the adatom covered Pt surface is only a small fraction of the number of potential adsorption sites on the bare Pt surface. This difference suggests that nucleation and 3-D growth involves only certain sites of the Hg-adatom layer where adsorbate and surface atom rearrangements become possible[23].

Acknowledgements—This work was supported by the Universidad Nacional de La Plata, the Consejo Nacional de Investigaciones Cientificas y Técnicas, the Comisión de Investigaciones Cientificas (Provincia de Buenos Aires). This work was partially supported by the regional program for the Scientific and Technological development of the Organization of the American States. Part of the equipment used in the present work was provided through the cooperation agreement between the University of Mainz (Germany). and the University of La Plata (Argentina). The authors thanks Lic. D. Margheritis for her participation in the early stages of the experimental work.

REFERENCES

1. L. A. Schadewald, T. R. Lindstrom, W. Hussein, E. E. Evenson and D. C. Johnson, *J. electrochem. Soc.* **131**, 1583 (1984).
2. M. Z. Hassan, D. Untereker and S. Bruckenstein, *J. electroanal. Chem.* **42**, 161 (1973).
3. S. P. Kounaves and J. Buffle, *J. electrochem. Soc.* **133**, 2495 (1986).
4. B. J. Bowles, *Nature* **212**, 1456 (1966).
5. S. Toschev, A. Milchev and S. Stoyanov, *J. Crystal Growth* **13/14**, 123 (1972).
6. S. Toschev and I. Markov, *Ber. Bunsenges Phys. Chem.* **73**, 184 (1969).
7. A. Milchev, E. Vassileva and V. Kertov, *J. electroanal. Chem.* **107**, 323 (1980).
8. A. Milchev, *Electrochim. Acta* **30**, 125 (1985).
9. R. Kaischev and B. Mutaftschiev, *Electrochim. Acta* **10**, 643 (1965).
10. A. Milchev and V. Tsakova, *Electrochim. Acta* **30**, 133 (1985).
11. V. Tsakova and A. Milchev, *J. electroanal. Chem.* **197**, 359 (1986).
12. A. Milchev, V. Tsakova, T. Chierchie, K. Juttner and W. J. Lorenz, *Electrochim. Acta* **31**, 971 (1986).
13. W. P. Lorenz, E. Schmidt, G. Staikov and H. Bort, *Faraday Symposia of the Chemical Society*, Vol. 12, p. 14 (1977).
14. S. Jaya, T. Prasada Rao and G. Prabhakara Rao, *ElectrochIm. Acta* **31**, 343 (1986).
15. R. C. Salvarezza, D. V. Vásquez Moll, M. C. Giordano and A. J. Arvia, *J. electroanal. Chem.* **213**, 301 (1986).
16. B. E. Conway, H. Angerstein-Kozlowska and W. A. Sharp, *Anal. Chem.* **45**, 1331 (1973).
17. B. Parajon Costa, N. R. de Tacconi, M. C. Giordano and A. J. Arvia, *J. electroanal. Chem.* (in press).
18. T. Chierchie, C. Mayer, K. Jüttner and W. J. Lorenz, *J. electroanal. Chem.* **191**, 401 (1985).
19. W. G. Sherwood and S. Bruckenstein, *J. electrochem. Soc.* **125**, 1099 (1978).
20. H. Bort, K. Juttner, W. J. Lorenz and G. Staikov, *Electrochim. Acta* **28**, 993 (1983).
21. G. Gunawardena, G. Hills and I. Montenegro, *Faraday Symposia of the Chemical Society*, Vol. 12, p. 90 (1977).
22. B. Scharifker and G. Hills, *Electrochim. Acta* **28**, 889 (1983).
23. D. Margheritis, R. C. Salvarezza, M. C. Giordano and A. J. Arvia, *J. electroanal. Chem.* **229**, 327 (1987).